

A NEW POPULATION OF HIGH- z , DUSTY Ly α EMITTERS AND BLOBS DISCOVERED BY WISE: FEEDBACK CAUGHT IN THE ACT?

CARRIE R. BRIDGE¹, ANDREW BLAIN², COLIN J. K. BORYS³, SARA PETTY⁴, DOMINIC BENFORD⁵, PETER EISENHARDT⁶,
DUNCAN FARRAH⁴, ROGER L. GRIFFITH³, TOM JARRETT⁷, CAROL LONSDALE⁸, SPENCER A. STANFORD⁹, DANIEL STERN⁶,
CHAO-WEI TSAI³, EDWARD L. WRIGHT¹⁰, AND JINGWEN WU^{6,10}

¹ California Institute of Technology, MS249-17, Pasadena, CA 91125, USA; bridge@astro.caltech.edu

² Department of Physics and Astronomy, University of Leicester, LE1 7RH Leicester, UK

³ Infrared Processing and Analysis Center, California Institute of Technology, MS 100-22, Pasadena, CA 91125, USA

⁴ Department of Physics, Virginia Polytechnic Institute and State University, Blacksburg, VA 24061, USA

⁵ NASA Goddard Space Flight Center, Greenbelt, MD 20771, USA

⁶ Jet Propulsion Laboratory, California Institute of Technology, 4800 Oak Grove Dr., Pasadena, CA 91109, USA

⁷ Astronomy Department, University of Cape Town, Rondebosch 7701, South Africa

⁸ National Radio Astronomy Observatory, 520 Edgemont Road, Charlottesville, VA 22903, USA

⁹ Department of Physics, University of California Davis, One Shields Ave., Davis, CA 95616, USA

¹⁰ Astronomy Department, University of California Los Angeles, Los Angeles, CA 90095, USA

Received 2012 October 18; accepted 2013 April 2; published 2013 May 7

ABSTRACT

By combining data from the NASA *Wide-field Infrared Survey Explorer* (WISE) mission with optical spectroscopy from the W. M. Keck telescope, we discover a mid-IR color criterion that yields a 78% success rate in identifying rare, typically radio-quiet, $1.6 \lesssim z \lesssim 4.6$ dusty Ly α emitters (LAEs). Of these, at least 37% have emission extended on scales of 30–100 kpc and are considered Ly α “blobs” (LABs). The objects have a surface density of only $\sim 0.1 \text{ deg}^{-2}$, making them rare enough that they have been largely missed in deep, small area surveys. We measured spectroscopic redshifts for 92 of these galaxies, and find that the LAEs (LABs) have a median redshift of 2.3 (2.5). The WISE photometry coupled with data from *Herschel* (*Herschel* is an ESA space observatory with science instruments provided by European-led Principal Investigator consortia and with important participation from NASA) reveals that these galaxies are in the Hyper Luminous IR galaxy regime ($L_{\text{IR}} \gtrsim 10^{13}\text{--}10^{14} L_{\odot}$) and have warm colors. They are typically more luminous and warmer than other dusty, $z \sim 2$ populations such as submillimeter-selected galaxies and dust-obscured galaxies. These traits are commonly associated with the dust being illuminated by intense active galactic nucleus activity. We hypothesize that the combination of spatially extended Ly α , large amounts of warm IR-luminous dust, and rarity (implying a short-lived phase) can be explained if the galaxies are undergoing brief, intense “feedback” transforming them from an extreme dusty starburst/QSO into a mature galaxy.

Key words: galaxies: formation – galaxies: high-redshift – galaxies: ISM – galaxies: starburst – infrared: galaxies

Online-only material: color figures

1. INTRODUCTION

High-redshift Ly α emission is widely used to study star formation in galaxies (e.g., Cowie & Hu 1998; Steidel et al. 2000; Gawiser et al. 2007; Gronwall et al. 2007; Nilsson et al. 2007; Finkelstein et al. 2009; Ono et al. 2010). Systems that exhibit this line are typically referred to as Ly α emitters (LAEs); a small subset show extended emission on scales $\gtrsim 30$ kpc (occasionally upward of 100 kpc) and are considered Ly α “blobs” (LABs). Among the largest coherent galactic structures known in the universe, LABs are extremely energetic, with Ly α luminosities of $\sim 10^{42}\text{--}10^{44} \text{ erg s}^{-1}$, and have been shown to trace over-densities of galaxies at high-redshift (e.g., Keel et al. 1999; Francis et al. 2001; Steidel et al. 2000; Matsuda et al. 2004; Prescott et al. 2008, 2012a; Yang et al. 2009; Erb et al. 2011). Bright, optically selected LABs are 100–1000 times less abundant than LAEs (e.g., Steidel et al. 2000; Matsuda et al. 2004; Saito et al. 2006) with only a few dozen known (Steidel et al. 2000; Matsuda et al. 2004, 2011; Dey et al. 2005; Geach et al. 2005; Nilsson et al. 2006; Lai et al. 2007; Smith & Jarvis 2007; Prescott et al. 2009, 2012b; Yang et al. 2009, 2010; Ouchi et al. 2009; Webb et al. 2009).

Resonant scattering by atomic hydrogen means Ly α photons are easily extinguished by dust. This suggests that dusty infrared

galaxies and LAE/LAB populations, despite both peaking in activity around $z \sim 2$, should largely not overlap. Indeed *Spitzer* observations of ~ 40 optically selected $z = 2\text{--}3.5$ LABs found that only $\lesssim 15\%$ are also luminous in the infrared (Webb et al. 2009). Furthermore, no known optically discovered LAB is WISE detected at 12 or 22 μm (see Section 3.1 of this work) including the first LAB found through its dust emission at 24 μm (Dey et al. 2005). Although, 40%–50% of the infrared luminous submillimeter galaxies (SMGs) show Ly α emission, they rarely exhibit spatially extended Ly α emission (Chapman et al. 2005). This suggests however, that dust and Ly α emission are not in fact mutually exclusive, and points to a clumpy dust distribution that allows sight lines for Ly α photons to escape (Neufeld 1991). Since SMGs and related high-redshift galaxies are thought to be just one stage in the evolution of massive elliptical galaxies, the study of spatially extended Ly α in dusty galaxies can thus provide a unique insight into this process.

This discovery paper is the first in a series, and presents a new and efficient mid-IR color technique to select a never before seen population of $z \sim 2\text{--}4$ dusty LAEs, of which at least one-third are also found to be LABs. We use the redshift distribution, general spectroscopic properties, and preliminary *Herschel* observations to determine how these objects relate to other dusty galaxies at these redshifts and speculate how these enormous

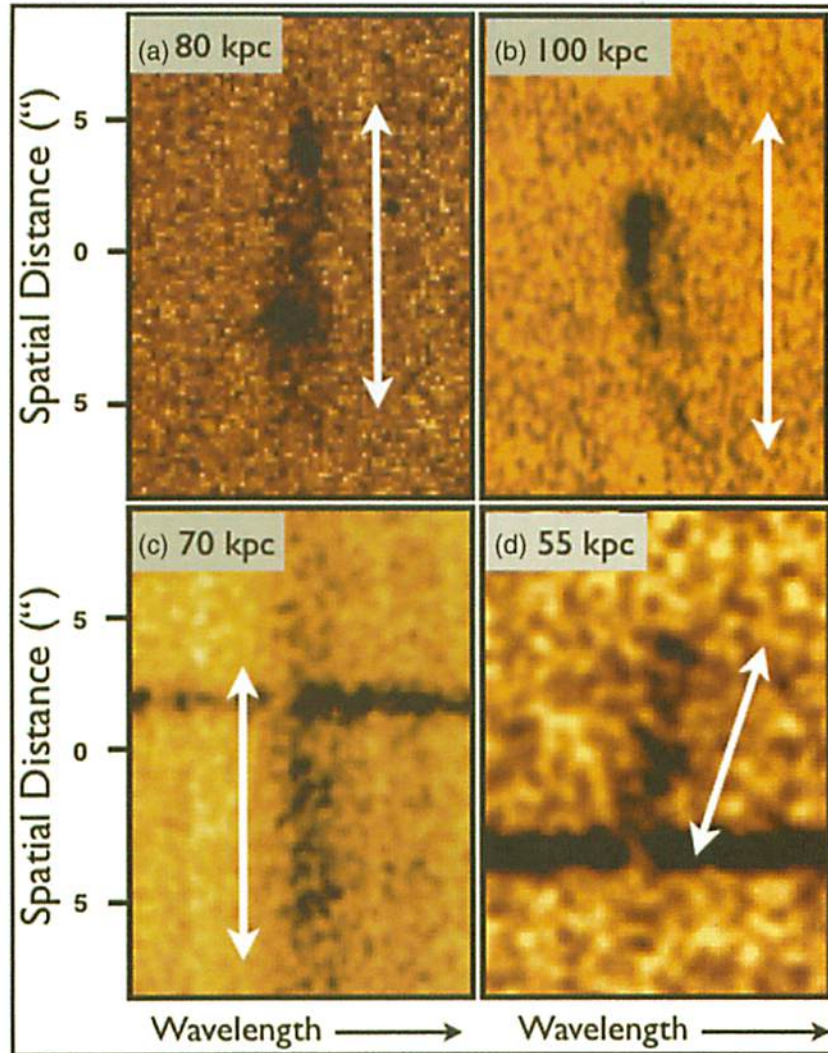


Figure 1. Two-dimensional LRIS spectra for four of the WLABs. The spatial extent of the Ly α emission is noted in the corner of each image. These examples are representative of the asymmetric, spatially extended line profile, and clumpy nature of the Ly α emission found in these galaxies. The arrows are meant to guide the eye and highlight the variation in velocity profiles.

(A color version of this figure is available in the online journal.)

LABs are being powered. We assume a Λ CDM cosmology with $\Omega_M = 0.27$, $\Omega_\Lambda = 0.73$, and $H_0 = 71 \text{ km s}^{-1} \text{ Mpc}^{-1}$ and use Vega magnitudes.

2. SAMPLE DEFINITION AND OBSERVATIONS

One of the primary science goals of the NASA *Wide-field Infrared Survey Explorer* (*WISE*) mission (Wright et al. 2010), which covers the whole sky at wavelengths of 3.4, 4.6, 12, and 22 μm (W1–W4), is to find the most luminous galaxies in the universe. We performed initial searches in *WISE* color space which revealed a diversity of galaxy types over a wide range of redshifts (Griffith et al. 2011; Eisenhardt et al. 2012; Wu et al. 2012; Lonsdale et al. 2013; C. R. Bridge et al. 2013, in preparation). In this discovery paper we report the results of a deep spectroscopic follow-up campaign to target optically faint galaxies with the reddest *WISE* (mid-IR) colors. A striking finding of this work is that not only did the majority of these high-redshift sources have intense Ly α emission at least one-third of these *WISE*-selected LAEs are LABs, having spatially extended Ly α reaching 30–100 kpc (see Figure 1).

We refer to this new population of hot, dusty, *WISE*-detected LAEs/LABs as—WLAEs and WLABs because they are selected by *WISE* colors, and cover a previously unexplored wavelength and flux density parameter space over the whole sky.

2.1. Selection Method

Realizing that WLAEs and WLABs lie in a very specific region of a *WISE* color–magnitude diagram, we refined the selection criteria used in the initial spectroscopic follow-up to focus on high-redshift LAEs/LABs.

The resulting “WLAB” selection criteria, shown in Figure 2, requires $W2-W3$ ($4.5-12 \mu\text{m}$) ≥ 4.8 and $S/N \geq 5$ in W3 and W4. We also excluded sources within 30° of the Galactic center and 10° of the Galactic plane to avoid asymptotic giant branch stars and saturation artifacts. In order to remove low-redshift ($z \lesssim 0.5$) star-forming galaxies with similar *WISE* colors, we required non-detections in Sloan Digital Sky Survey and Digitized Sky Survey imaging ($r' \gtrsim 22$). Finally, each object’s co-added W3 and W4 images were visually inspected to ensure the source is not spurious. These criteria result in an average source density of $\sim 0.1 \text{ deg}^{-2}$.

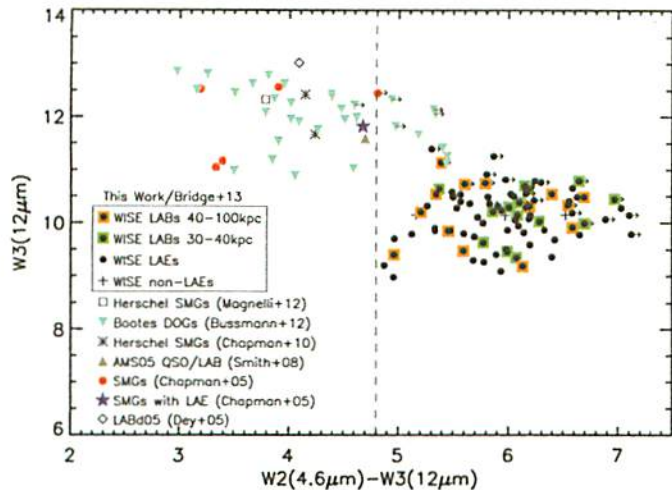


Figure 2. *WISE* W3(12 μm) vs. *WISE* W2–W3 (4.5–12 μm) color for all sources in the sample with spectroscopic redshifts between $1.6 \leq z \leq 4.6$. WLAEs (black circles), 30–40 kpc WLABs (green squares), and 40–100 kpc WLABs (orange squares) are plotted. For comparison, $z = 2$ –3 *WISE* detected SMGs/DOGs are highlighted: Magnelli et al. (2012, open squares), Bussmann et al. (2012, cyan downward triangle), Chapman et al. (2010, black asterisks), Smith et al. (2009, gray triangle), Chapman et al. (2005, red circle), and Chapman et al. (2005, blue star). LABd05 is not detected by *WISE*, hence the data shown is from *Spitzer* (Dey et al. 2005). The WLAEs (WLABs) exhibit unique, redder mid-IR colors (implying hotter dust temperatures) than other dusty $z \sim 2$ populations. The WLAE/WLAB selection technique has a 78% (>29%) success rate in identifying $z > 1.6$ dusty LAEs (LABs).

(A color version of this figure is available in the online journal.)

2.2. Optical Spectroscopy

To determine redshifts and discern the nature of the galaxies, we used Keck I LRIS (Oke et al. 1995) over the course of six runs between 2010 July and 2012 January. The sample contains 101 objects that fulfill the WLAE/WLAB selection, of which close to half had previously been followed-up using other red selections (i.e., W1W2-drop criteria; Eisenhardt et al. 2012) and therefore did not need to be re-observed. The full spectroscopic campaign will be presented in an upcoming paper. The majority of data were taken using the $600 \ell \text{ mm}^{-1}$ grism in the blue arm ($\lambda_{\text{blaze}} = 4000 \text{ \AA}$; spectral resolving power $R \equiv \lambda/\Delta\lambda \sim 750$), the $400 \ell \text{ mm}^{-1}$ grating on the red arm ($\lambda_{\text{blaze}} = 7800 \text{ \AA}$; $R \sim 700$), the 5600 \AA dichroic and a $1''.5$ wide long slit. The targets were observed with a median seeing of $0''.7$ with total integration times between 20–40 minutes. The LRIS data were reduced and flux calibrated using standard procedures.

The optical spectroscopy reveals a wide range of characteristics, from pure starburst galaxies with narrow emission lines and several ultraviolet interstellar absorption lines comparable to Lyman break galaxies (Steidel et al. 2000) to those with strong active galactic nucleus (AGN) components, inferred from the presence of high ionization lines such as N v, Si IV/O IV, C IV and broad emission line profiles of several thousand km s^{-1} .

Robust redshifts based on two or more spectral features (primarily N v, Si IV/O IV, C IV, Mg II, He II) were determined for 92 out of the 101 sources we targeted (91% success rate), while the remaining 9 showed no continuum or spectral lines. We believe these nine sources are most likely highly dust-obscured and hence below our detection threshold. The sample has a redshift range of $z = 1.13$ – 4.59 (see Figure 3). The *WISE* LAEs (LABs) have a roughly Gaussian redshift distribution centered around $z = 2.5$ (2.3). The excellent blue sensitivity of LRIS allows Ly α emission to be detected down to 3160 \AA ,

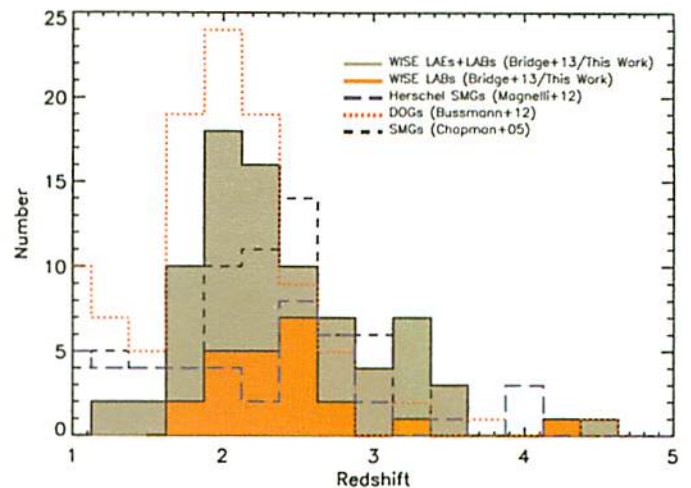


Figure 3. Spectroscopic redshift distribution for the full sample (WLAEs+WLABs; filled gray), and WLABs (filled orange). For comparison we plot the redshift distribution of other well-studied dusty populations: SMGs (black dashed; Chapman et al. 2005), *Herschel* SMGs (blue long dashed; Magnelli et al. 2012), and DOGs (red dotted; Bussmann et al. 2012). The *WISE* LAEs (LABs) have a roughly Gaussian redshift distribution centered around $z = 2.5$ (2.3), very similar to that of SMGs and DOGs.

(A color version of this figure is available in the online journal.)

corresponding to a redshift of $z \sim 1.6$. Of the 92 *WISE*-selected galaxies with a robust redshift, 3 were $z < 1.6$ star-forming galaxies, while 89 were at a $z \geq 1.6$, and of those 79 (89%) showed Ly α in emission. Given all of the spectra exhibited multiple emission lines (typically Ly α , N v, C IV), a secure identification of Ly α was possible. An additionally striking finding was that 37% (29/79) of the WLAEs showed Ly α emission in the two-dimensional spectra extended on spatial scales of ≥ 30 kpc, with 18% (14) having emission 40–100 kpc in extent (i.e., LABs).

Given we used random slit orientations the detection rate is consistent with all the LAEs in our sample being LABs. We also note that an additional 14 (of the 79 WLAEs) have extended emission of 25–30 kpc, which is more than twice the seeing and 4–5 times the typical sizes of dusty $z \sim 2$ galaxies (i.e., SMGs and dust-obscured galaxies (DOGs); Chapman et al. 2005; Biggs & Ivison 2008; Bussmann et al. 2009; Casey et al. 2009; Iono et al. 2009; Bothwell et al. 2010; Younger et al. 2010). These therefore constitute smaller LABs or Ly α clouds.

The definition of a LAB does vary between studies. Matsuda et al. (2004) required an isophotal area of at least 16 arcsec^2 (or ~ 30 kpc in length at $z = 3.1$) and a surface brightness of $\sim 27.6 \text{ mag arcsec}^{-2}$ ($\sim 2 \times 10^{-18} \text{ erg s}^{-1} \text{ cm}^{-2} \text{ arcsec}^{-2}$), while Matsuda et al. (2011) probed down to $1.4 \times 10^{-18} \text{ erg s}^{-1} \text{ cm}^{-2} \text{ arcsec}^{-2}$. In contrast to these narrow-band imaging studies we used the one-dimensional spectra to measure the spatial extent of the Ly α emission in one direction. Multiple slit orientations were used to probe the spatial line morphology for four of the LABs. A slit position angle rotated by 45° and 90° of the original angle often showed little or no extended emission, implying an asymmetric and filamentary line morphology.

The depth of the spectroscopy reached Ly α surface brightnesses of 1 – $100 \times 10^{-18} \text{ erg s}^{-1} \text{ cm}^{-2} \text{ arcsec}^{-2}$. This is well within the range used in optical narrow-band surveys to identify LABs (e.g., Steidel et al. 2000; Matsuda et al. 2004, 2011; Nilsson et al. 2006; Smith & Jarvis 2007; Ouchi et al. 2009; Yang et al. 2009, 2010). Each WLAE spectra was inspected and

Table 1
Far-IR Properties of the Eight Objects with *Herschel* Observations

z	$S(70)$	$S(160)$	$S(250)$	$S(350)$	$S(500)$	T (K)	$\log(L/L_{\odot})$
2.022	27	80	63	52	43	52 ± 8	13.1 ± 0.1
2.140	84	217	172	110	53	70 ± 6	13.8 ± 0.1
2.298	40	75	109	82	44	46 ± 6	13.3 ± 0.1
2.450	18	60	62	41	<30	60 ± 7	13.2 ± 0.1
2.452	29	53	47	33	<30	84 ± 8	13.4 ± 0.1
2.542	24	40	39	34	<30	84 ± 12	13.3 ± 0.1
3.048	8	37	59	56	43	48 ± 3	13.3 ± 0.1
3.228	16	56	53	45	<30	71 ± 10	13.5 ± 0.1

Notes. Flux errors (1σ) for the *Herschel* bands are 4, 10, 6, 6, 8 mJy corresponding to 70, 160, 250, 350, and 500 μm . Dust temperature and luminosity were fit using a gray body with $S(\nu) \propto B(\nu)\nu^{1.5}$, where $B(\nu)$ is the Planck function and the statistical 1σ errors are quoted.

those with spatially extended Ly α emission $\gtrsim 30$ kpc were classified as *WISE* LABs or WLABs. Given that the Ly α surface brightness reached by the spectra conservatively satisfy, and in many cases are brighter than the definitions of traditional LABs, it is highly plausible that the true sizes of the WLABs are in fact larger under these standard definitions. The sizes of the individual WLABs and their line fluxes will be presented in depth in the catalog paper (C. R. Bridge et al. 2013, in preparation). Applying the LAE (LABs) fractions found by our spectroscopic survey to the total number of sources that satisfy the color criteria we estimated a source density for WLAEs (WLABs) of ~ 0.1 (0.03) deg^{-2} , or approximately 4500 (1600) over the full sky.

2.3. Far-infrared Photometry

The red *WISE* colors strongly argue that significant amounts of warm dust are present in these galaxies. Since the spectral energy distributions (SEDs) of dusty galaxies typically peak in the far-infrared, observations between 0.1–1 mm are required in order to accurately determine the total IR luminosity and dust temperature of the sources. To that end, we have undertaken a campaign with *Herschel* to study the WLABs in five bands covering 70–500 μm using the PACS (Poglitsch et al. 2010) and SPIRE (Griffin et al. 2010) imagers.

Eight objects with *WISE* colors drawn randomly from our selection have been observed with *Herschel* to date, and all were detected in at least four bands (see Table 1). To estimate the dust luminosity and temperature, these data were fit using a modified blackbody with $S(\nu) \propto B(\nu, T)\nu^{1.5}$. Here, $B(\nu, T)$ is the Planck function.

While more complex models can be used, this parameterization has been adopted by many other studies, enabling a straightforward comparison with, for example, samples of SMGs and DOGs presented in Magnelli et al. (2012) and Melbourne et al. (2012), respectively. Figure 4 presents the results of these fits and indicates that WLABs typically contain warmer dust than these other samples. This suggests that they are being heated, at least in part, by an AGN, since starburst galaxies such as SMGs are typically colder (also see Wu et al. 2012). The WLABs are systematically more luminous than SMGs, with bolometric luminosities in excess of $L_{\text{FIR}} > 10^{13} L_{\odot}$, making them Hyper-Luminous Infrared Galaxies (HyLIRGs).

It is tempting to associate these high luminosities with gravitational lensing; however, none of the optical spectra demonstrate contamination from a foreground source, and the

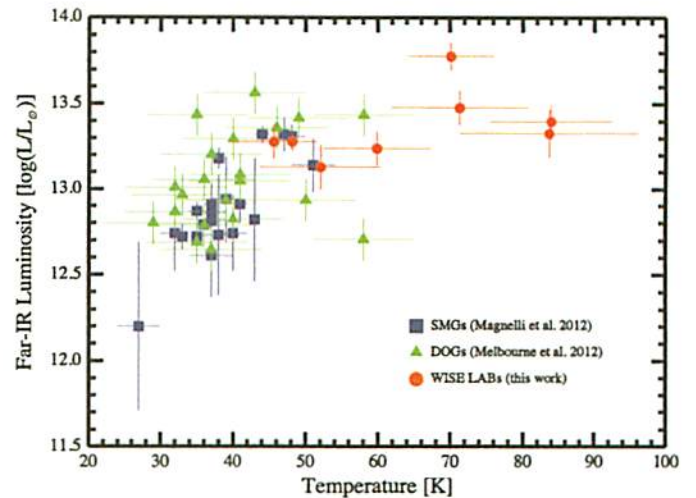


Figure 4. Estimated dust properties based on *Herschel* observations. Objects between $2.0 \leq z \leq 3.5$ extracted from catalogs of DOGs and unlensed SMGs are plotted against the eight observed WLABs which cover a similar redshift range. In all cases, fits are to a single temperature modified blackbody, with a fixed emissivity of $\beta = 1.5$. Error bars in all cases are based on fit results only and do not account for other systematic effects.

(A color version of this figure is available in the online journal.)

spatially extended Ly α emission for all the sources is at the same redshift as the other spectral features. Furthermore, visual inspection of near-IR, adaptive optic (AO) imaging with Keck’s NIRC2 camera (Eisenhardt et al. 2012; C. R. Bridge et al. 2013, in preparation), and *Hubble Space Telescope* WFC3/IR imaging of over a dozen WLABs (C. R. Bridge et al. 2013, in preparation) reveal no evidence of either a potential lens (nearby galaxies or clusters) or any morphological signatures, such as arcs or multiple components that the *WISE* object itself is lensed. However a full lensing analysis is required to rule out any small amplifications.

3. DISCUSSION

3.1. *WISE* LABs and Previously Known LABs

One of the main features that sets this new population of WLAEs apart from other high-redshift galaxies, aside from their extremely red mid-IR color, is the unprecedented fraction that exhibit spatially extended Ly α emission, despite having large amounts of dust. Traditionally, LABs have been discovered serendipitously through narrow-band optical surveys that concentrate on a particular redshift (e.g., Steidel et al. 2000; Matsuda et al. 2004, 2011; Nilsson et al. 2006; Smith & Jarvis 2007; Yang et al. 2009, 2010; Ouchi et al. 2009), and more recently using optical broad-band surveys (Prescott et al. 2012b, 2013). These types of surveys more closely resemble “blind” searches, in that there is no a priori knowledge of where or how many LABs reside in the field. In contrast, the technique presented here (Figure 2) uses broad-band photometric data alone to preselect with high efficiency a population of LABs over a wider range of redshifts, with the caveat that they are seemingly much dustier than the ones found in optical surveys.

Although WLABs, at the correct redshift, would be detected in most optical narrow-band LAB searches, this type of serendipitous methodology can only efficiently patrol a small area, from a few square arcmins up to a couple of square degrees of the sky (Steidel et al. 2000; Matsuda et al. 2004, 2011). Given a WLAB surface density of 0.03 deg^{-2} , the WLABs are thousands of times rarer than their optical LAB cousins,

meaning that we should not have expected to discover any WLABs in existing optical LABs surveys. Again, this is consistent with our finding, that no optical LAB has the extreme mid-IR colors exhibited by the WLABs. We proceed now with the details of that investigation.

We cross matched the WISE catalog with *all* previously known LABs in the literature (Steidel et al. 2000; Matsuda et al. 2004, 2011; Dey et al. 2005; Geach et al. 2005; Nilsson et al. 2006; Lai et al. 2007; Smith & Jarvis 2007; Prescott et al. 2009, 2012b; Yang et al. 2009, 2010; Ouchi et al. 2009; Smith et al. 2009; Webb et al. 2009) and found that *none* are detected at 12 or 22 μm above a S/N of 5. It is important to note that this includes all published LABs known to have mid- or far-IR detections from follow-up observations with *Spitzer* and *Herschel* (Geach et al. 2005; Dey et al. 2005; Webb et al. 2009). No previously known LABs, including those which exhibit IR emission, are *WISE* sources, and would not be selected by the WLAB color technique. It is clear that WLABs occupy a distinct region of mid-IR color space, and are likely in a different stage of evolution, environment, or energy generation process (i.e., AGN, extreme starburst) than previously discovered LABs.

Despite the WLABs being a factor of 10–1000 times more luminous in the mid–far-IR than any previously discovered LAB, they have $\text{Ly}\alpha$ luminosities (10^{42} – 10^{44} erg s^{-1}), rest-frame equivalent widths (a few tens to 300 \AA), and LABs sizes similar to those discovered optically. In other words, in the optical WLABs are similar to LABs but they have a larger fraction of mid-IR power to $\text{Ly}\alpha$ emission. We hypothesize that the success of the WLAB technique is due to it being able to select AGN at or near its peak of energy output. Such an object could produce strong outflows clearing paths through the dust for the $\text{Ly}\alpha$ photons to escape. Indeed our optical spectra do exhibit lines consistent with a strong outflow (see Section 3.3 for a discussion). While supernovae (SNe) are also thought to provide a mechanism for clearing out dust, a powerful starburst alone cannot account for the strong mid-IR luminosities, red colors or hot (50–85 K) dust temperatures (Section 2.3 and Table 1) displayed by these systems. Additionally, SMGs, which demonstrate similar levels of star formation do not exhibit extended $\text{Ly}\alpha$ emission. Therefore, intense star formation is likely not the primary process responsible for the WLABs.

It is worth reiterating that the phenomena of large $\text{Ly}\alpha$ halos has also been found around some high-redshift radio galaxies (HzRGs) and QSOs (e.g., McCarthy et al. 1987; Heckman et al. 1991; Reuland et al. 2003; Smith et al. 2009). In these systems the extended $\text{Ly}\alpha$ emission is thought to be powered by interactions between the radio jets and the ambient intergalactic medium (IGM). The majority (two-thirds) of our sources are undetected in the FIRST (<1 mJy) or NVSS radio surveys, and while one-third do show faint radio fluxes they are well off the $\text{Ly}\alpha$ -radio correlation (in both $\text{Ly}\alpha$ and radio flux) found for HzRGs (Smith et al. 2009), differentiating them from this well-studied population. However it may be the case that the WLABs are in a radio quiet stage and may evolve into similar systems.

3.2. WLABs and Other Dusty High-redshift Populations

Though the IR luminosity and redshift distribution of the WLAEs/WLABs are similar to other populations of IR-luminous galaxies (Figure 3), they must differ in some way given the large fraction with extended $\text{Ly}\alpha$ emission.

Blind submillimeter surveys have been very successful at finding high-redshift, dust-obscured galaxies with far-IR

luminosities in excess of $10^{12} L_{\odot}$ (i.e., SMGs; e.g., Smail et al. 1997; Barger et al. 1999; Blain et al. 1999; Borys et al. 2005; Hainline et al. 2009). However, these long wavelength observations ($\gtrsim 500 \mu\text{m}$) select systems with cooler dust and less extreme mid-IR colors than seen in our *WISE* sample (Figures 2 and 4). Generally, SMGs are powered by star formation rather than Compton-thin AGN (Alexander et al. 2005). Based on the limited *Herschel* observations conducted so far, most of the WLABs would also be classified as SMGs. However only 1%–2% of known SMGs fulfill the WLAE/WLAB color criteria (this work; Figure 2), and there are only a couple of rare SMGs with extended $\text{Ly}\alpha$ emission (Chapman et al. 2005).

Dey et al. (2008) have successfully used a mid-IR to optical flux ratio ($F_{24\mu\text{m}}/F_R > 1000$ and $F_{24\mu\text{m}} > 0.3$ mJy) to select a population of $z \sim 2$ dust-obscured galaxies, which they refer to as DOGs (Houck et al. 2005; Desai et al. 2009; Bussmann et al. 2012). By probing blueward of the SED peak, this technique recovers a mix of AGN and starburst dominated galaxies the majority of which reside at $z \sim 2$. Given that DOGs share a common epoch, dusty composite nature and mid-IR selection it makes sense to briefly compare them to the WLAEs/WLABs. The DOG sample from Bussmann et al. (2012) was cross checked with the WISE catalog and revealed that only $\sim 8\%$ of the DOGs ($N = 8$) fulfill the WLAE/WLAB selection presented here. Although there is some overlap in the W2–W3 color space, Figure 2 highlights that *Spitzer* DOGs are typically 1.5–2 mag fainter at 12 μm (W3) than the WLAEs/WLABs. Deep optical spectroscopy of $\sim 60\%$ of these *Spitzer* DOGs has been conducted by Bussmann et al. (2012) and one source has been reported to exhibit extended $\text{Ly}\alpha$ (Dey et al. 2005), however it is not detected by *WISE* and is more akin in mid-IR flux to a traditional SMG. The fainter W3 flux of *Spitzer* DOGs could reflect a lower intrinsic luminosity (also see Figure 4) or a different nature. Using the observed r' –W4 color of the WLAEs/WLABs, we also consider the fraction that would satisfy the DOG criterion. All our WLAEs/WLABs would be classed as DOGs, although they are too rare to have been discovered in *Spitzer* MIPS 24 surveys. Finally, it is important to note that the DOG criterion focuses purely on the optical-to-mid-IR flux ratio, and does not specifically select sources with a steeply rising mid-IR SED (Figure 2), which is what we have shown are generally the objects that exhibit extreme $\text{Ly}\alpha$ properties.

It is also important to discuss the similarities and differences between the WLAE/WLAB selection and other *WISE*-based color selections that have been undertaken. One such example is the “W1W2-dropouts,” outlined in Eisenhardt et al. (2012), which has been successful in identifying ULIRGs over a wider redshift range ($z \sim 0.05$ –4.6). There is a substantial overlap in the $z \gtrsim 2$ samples; however, overall we find that the refined WLAE/WLAB criterion is twice as effective at selecting WLAE/WLABs at high- z . The primary differences between these two selections are that the WLAE/WLAB criteria impose an optical magnitude limit to remove contamination from low redshift galaxies, places no flux cut on W1 (many WLABs are detected in W1 and/or W2), probe a factor of 1.2 (2) deeper in W3 (W4) flux and are 0.5 mag bluer in W2–W3 than the W1W2-dropout selection.

Another *WISE* extragalactic color selection presented in Lonsdale et al. (2013), combines specific *WISE* colors, with the requirement of an intermediate or loud radio detection in the regions of sky covered by the NVSS 20 cm radio survey (Condon et al. 1998). Although these sources share similarly

red mid-IR colors to that of the WLAE/WLAB population the redshift range of these red radio sources is systematically lower ($z \sim 0.4\text{--}2.5$; Lonsdale et al. 2013) and they show no evidence of extended Ly α . As suggested in Lonsdale et al. (2013), these red-radio loud objects are good candidates for being in a QSO-dominated phase. It is possible that some of the powerful AGN thought to reside in both the WLABs and these red-radio loud sources are merely at different stages of their evolution. We will discuss the potential connection between these and the other populations mentioned above in more detail in the WLAB catalog paper (C. R. Bridge et al. 2013, in preparation).

3.3. Spectral Properties of WISE LABs

The cause of the LAB phenomena in optically selected samples is still an outstanding question (e.g., Nilsson et al. 2006; Prescott et al. 2009, 2012a; Yang et al. 2009, 2010; Colbert et al. 2011). A logical explanation is photo-ionization by an embedded source, however Matsuda et al. (2004) showed that many LABs do not house a sufficiently UV-bright galaxy. Optically discovered LABs, like the WISE LABs are radio-quiet and hence are not powered by interactions between radio-jets and the ambient IGM as in the case of the Ly α halos surrounding HzRGs (e.g., McCarthy et al. 1987; Heckman et al. 1991; Reuland et al. 2003; Smith et al. 2009). Alternative mechanisms are (1) cold accretion, where the LABs are powered by gravitational heating during the collapse of a large primordial cloud (Haiman et al. 2000; Kereš et al. 2005; Dijkstra et al. 2006; Dekel & Birnboim 2006; Nilsson et al. 2006; Smith & Jarvis 2007; Smith et al. 2008), (2) intense starbursts or and embedded AGN (e.g., Keel et al. 1999), (3) shocks from SN winds or AGN outflows (e.g., Geach et al. 2005; Colbert et al. 2011), and (4) resonant scattering of Ly α photons (e.g., Steidel et al. 2011; Saito et al. 2006). Given that all the WLABs are associated with a luminous IR galaxy and less than 15% of optical LABs are (Webb et al. 2009), suggests that the dominant powering mechanisms behind these two species of LABs are likely different. For clues we investigate the optical spectra.

The high-ionization and broad emission lines seen in $\gtrsim 70\%$ of optical spectra suggest that the majority, if not all, of the WLAEs/WLABs host a dust-obscured AGN, which is also consistent with the *Herschel* and *WISE* colors. The Ly α emission is spatially asymmetric and clumpy, and is often offset from the systemic redshift of the galaxy by 100–1000's of km s^{-1} , implying large-scale outflows. Furthermore, many galaxies in the sample demonstrate velocity structure in the Ly α line, redshifted up to several thousand km s^{-1} as a function of distance from the central component (Figure 1(d)). The line profiles are diverse, ranging from traditional P-Cygni profiles characteristic of Wolf–Rayet and O-star winds to Ly α emission peaking on the blue side of the Ly α profile, suggesting possible inflows (Dijkstra & Loeb 2009; Barnes et al. 2011).

The filamentary morphology of the extended Ly α seen when multiple slit orientations were used suggests that the quoted efficiency of the color selection in identifying LABs is a lower limit. Indeed, using a simple model of the extended emission size, geometry, and random slit orientation the 37% detection rate is consistent with all the LAEs in our sample being LABs.

The diversity of spectral properties can be explained by either varying levels of dust extinction or perhaps the systems are at slightly different stages of evolution.

3.4. WISE LABs: AGN Feedback Caught in the Act?

The correlation between the masses of supermassive black holes (SMBH) at the center of nearby ellipticals and their bulge stellar velocity dispersion remains striking in the study of galaxy evolution (e.g., Ferrarese & Merritt 2000). The general paradigm that ties these passive galaxies with their high-redshift progenitors is a process of merger-induced star formation which also fuels the SMBH (e.g., Sanders & Mirabel 1996; Hopkins et al. 2006). The system appears at one point as a heavily obscured star-forming galaxy, and later, as the SMBH accretes at a higher rate, a galaxy with an active nucleus. AGN- and starburst-induced winds eventually become strong enough to expel the obscuring gas and dust, briefly revealing an optical quasar. This short-lived “feedback” process is thought to quench both star formation and AGN activity, leading ultimately to a passive, red galaxy spheroid (e.g., Hopkins et al. 2006; Farrah et al. 2012). Observational evidence for this process has been challenging to obtain, but models provide a general picture of the properties of these systems.

It is well established that the peak of this feedback activity occurs near $z \sim 2$ (e.g., Di Matteo et al. 2005), and that a multitude of galaxy types are associated with the process. SMGs are thought to be the IR-luminous starbursting precursors to systems that will evolve into a massive elliptical, and have been well characterized in a number of studies (e.g., Blain et al. 1999; Chapman et al. 2005; Magnelli et al. 2012).

Using a three-dimensional radiative equilibrium code, Chakrabarti et al. (2007) predict *Herschel* colors for systems undergoing feedback from SN and AGN feedback separately and showed that AGN feedback alone is particularly effective at dispersing gas and dust. They predict that for a brief time (< 40 Myr) while the AGN injects energy into the galaxy and surrounding IGM at its maximal rate, the dust is hotter than during the SMG starburst phase. SMGs (including the “warm” SMGs discovered by *Herschel*) typically have far-IR colors consistent with only SN feedback, while all the WLABs have *Herschel* colors ($F_{110\mu\text{m}}/F_{170\mu\text{m}}$) at least twice as red (~ 0.6), in line with the model predictions for when AGN feedback is at or near its peak. While Chakrabarti et al. (2007) does not make predictions regarding the Ly α morphology, other models do predict that given a clumpy gas and dust distribution, the Ly α would also likely not be symmetrical which is consistent with the filamentary Ly α we have observed (Cen & Zheng 2012). However, more detailed modeling is required.

Finally, the surface density of WLABs is generally consistent with predicted numbers of HyLIRGs from models (e.g., Béthermin et al. 2011) coupled with timescale arguments for the feedback process and length of the SMG phase. However we caution that this is not a particularly strong argument given the uncertainty in these models as well. Nevertheless, the accumulated evidence suggesting that the WLABs are undergoing extremely powerful feedback is intriguing, and we will expand on it in future papers.

4. CONCLUSIONS AND FUTURE WORK

This discovery paper presents a new *WISE* color criterion with a 78% success rate in selecting $z = 1.6\text{--}4.6$ dusty, mid-IR bright, LAEs, of which at least 37% (perhaps all) are LABs. This new population of rare ($\sim 0.1 \text{ deg}^{-2}$) galaxies, previously missed in narrow-area surveys, have a redshift distribution that peaks at $z \sim 2.3$, and total IR luminosities and dust temperatures on average brighter and hotter than SMGs and other high-redshift

dusty galaxies. This is the first systematic search technique to highlight bright, extremely dusty (hot) LAEs/LABs, and unlike optical narrow-band searches covers a large redshift range, the whole sky, and without contamination by low redshift interlopers (i.e., mistaking [O II] for Ly α) making it well suited to providing targets for future large spectroscopic surveys.

The current evidence suggests that these galaxies are in a short-lived transition between dusty starburst and an optical QSO driven by the central AGN. If true, these systems offer a unique opportunity to investigate AGN feedback and how it can effect not only the galaxy but also the surrounding IGM. A full census of the optical spectroscopy, mid-far-IR properties, near-IR morphologies and catalog of the WLAEs/WLABs will be presented in a series of forthcoming papers.

The authors would like to thank the anonymous referee for suggestions that improved the clarity of this paper. This publication makes use of data products from the *Wide-field Infrared Survey Explorer*, a joint project of the University of California, Los Angeles, and the Jet Propulsion Laboratory/California Institute of Technology, funded by the National Aeronautics and Space Administration.

Some of the data presented herein were obtained at the W. M. Keck Observatory, which is operated as a scientific partnership among the California Institute of Technology, the University of California and the National Aeronautics and Space Administration. The Observatory was made possible by the generous financial support of the W. M. Keck Foundation.

The authors wish to recognize and acknowledge the very significant cultural role and reverence that the summit of Mauna Kea has always had within the indigenous Hawaiian community. We are most fortunate to have the opportunity to conduct observations from this mountain.

Facilities: WISE, Keck:I (LRIS), Herschel (PACS, SPIRE)

REFERENCES

- Alexander, D. M., Bauer, F. E., Chapman, S. C., et al. 2005, *ApJ*, 632, 736
 Barger, A. J., Cowie, L. L., & Sanders, D. B. 1999, *ApJ*, 518, L5
 Barnes, L. A., Haehnelt, M. G., Tesfari, E., & Viel, M. 2011, *MNRAS*, 416, 1723
 Béthermin, M., Dole, H., Lagache, G., Le Borgne, D., & Penin, A. 2011, *A&A*, 529, A4
 Biggs, A. D., & Ivison, R. J. 2008, *MNRAS*, 385, 893
 Blain, A. W., Kneib, J.-P., Ivison, R. J., & Smail, I. 1999, *ApJ*, 512, L87
 Borys, C., Smail, I., Chapman, S. C., et al. 2005, *ApJ*, 635, 853
 Bothwell, M. S., Chapman, S. C., Tacconi, L., et al. 2010, *MNRAS*, 405, 219
 Bussmann, R. S., Dey, A., Armus, L., et al. 2012, *ApJ*, 744, 150
 Bussmann, R. S., Dey, A., Lotz, J., et al. 2009, *ApJ*, 693, 750
 Casey, C. M., Chapman, S. C., Beswick, R. J., et al. 2009, *MNRAS*, 399, 121
 Cen, R., & Zheng, Z. 2012, *arXiv:1210.3600*
 Chakrabarti, S., Cox, T. J., Hernquist, L., et al. 2007, *ApJ*, 658, 840
 Chapman, S. C., Blain, A. W., Smail, I., & Ivison, R. J. 2005, *ApJ*, 622, 772
 Chapman, S. C., Ivison, R. J., Roseboom, I. G., et al. 2010, *MNRAS*, 409, L13
 Colbert, J. W., Scarlata, C., Teplitz, H., et al. 2011, *ApJ*, 728, 59
 Condon, J. J., Cotton, W. D., Greisen, E. W., et al. 1998, *AJ*, 115, 1693
 Cowie, L. L., & Hu, E. M. 1998, *AJ*, 115, 1319
 Dekel, A., & Birnboim, Y. 2006, *MNRAS*, 368, 2
 Desai, V., Soifer, B. T., Dey, A., et al. 2009, *ApJ*, 700, 1190
 Dey, A., Bian, C., Soifer, B. T., et al. 2005, *ApJ*, 629, 654
 Dey, A., Soifer, B. T., Desai, V., et al. 2008, *ApJ*, 677, 943
 Dijkstra, M., Haiman, Z., & Spaans, M. 2006, *ApJ*, 649, 37
 Dijkstra, M., & Loeb, A. 2009, *MNRAS*, 400, 1109
 Di Matteo, T., Springel, V., & Hernquist, L. 2005, *Natur*, 433, 604
 Eisenhardt, P. R. M., Wu, J., Tsai, C.-W., et al. 2012, *ApJ*, 755, 173
 Erb, D. K., Bogosavljević, M., & Steidel, C. C. 2011, *ApJ*, 740, L31
 Farrah, D., Urrutia, T., Lacy, M., et al. 2012, *ApJ*, 745, 178
 Ferrarese, L., & Merritt, D. 2000, *ApJ*, 539, L9
 Finkelstein, S. L., Rhoads, J. E., Malhotra, S., & Grogin, N. 2009, *ApJ*, 691, 465
 Francis, P. J., Williger, G. M., Collins, N. R., et al. 2001, *ApJ*, 554, 1001
 Gawiser, E., Francke, H., Lai, K., et al. 2007, *ApJ*, 671, 278
 Geach, J. E., Matsuda, Y., Smail, I., et al. 2005, *MNRAS*, 363, 1398
 Griffin, M. J., Abergel, A., Abreu, A., et al. 2010, *A&A*, 518, L3
 Griffith, R. L., Tsai, C.-W., Stern, D., et al. 2011, *ApJ*, 736, L22
 Gronwall, C., Ciardullo, R., Hickey, T., et al. 2007, *ApJ*, 667, 79
 Haiman, Z., Spaans, M., & Quataert, E. 2000, *ApJ*, 537, L5
 Hainline, L. J., Blain, A. W., Smail, I., et al. 2009, *ApJ*, 699, 1610
 Heckman, T. M., Lehnert, M. D., Miley, G. K., & van Breugel, W. 1991, *ApJ*, 381, 373
 Hopkins, P. F., Somerville, R. S., Hernquist, L., et al. 2006, *ApJ*, 652, 864
 Houck, J. R., Soifer, B. T., Weedman, D., et al. 2005, *ApJ*, 622, L105
 Iono, D., Wilson, C. D., Yun, M. S., et al. 2009, *ApJ*, 695, 1537
 Keel, W. C., Cohen, S. H., Windhorst, R. A., & Waddington, I. 1999, *AJ*, 118, 2547
 Kereš, D., Katz, N., Weinberg, D. H., & Davé, R. 2005, *MNRAS*, 363, 2
 Lai, K., Huang, J.-S., Fazio, G., et al. 2007, *ApJ*, 655, 704
 Lonsdale, C., et al. 2013, *ApJ*, in preparation
 Magnelli, B., Lutz, D., Santini, P., et al. 2012, *A&A*, 539, A155
 Matsuda, Y., Yamada, T., Hayashino, T., et al. 2004, *AJ*, 128, 569
 Matsuda, Y., Yamada, T., Hayashino, T., et al. 2011, *MNRAS*, 410, L13
 McCarthy, P. J., Spinrad, H., Djorgovski, S., et al. 1987, *ApJ*, 319, L39
 Melbourne, J., Soifer, B. T., Desai, V., et al. 2012, *AJ*, 143, 125
 Neufeld, D. A. 1991, *ApJ*, 370, L85
 Nilsson, K. K., Fynbo, J. P. U., Møller, P., Sommer-Larsen, J., & Ledoux, C. 2006, *A&A*, 452, L23
 Nilsson, K. K., Møller, P., Møller, O., et al. 2007, *A&A*, 471, 71
 Oke, J. B., Cohen, J. G., Carr, M., et al. 1995, *PASP*, 107, 375
 Ono, Y., Ouchi, M., Shimasaku, K., et al. 2010, *MNRAS*, 402, 1580
 Ouchi, M., Ono, Y., Egami, E., et al. 2009, *ApJ*, 696, 1164
 Poglitsch, A., Waelkens, C., Geis, N., et al. 2010, *A&A*, 518, L2
 Prescott, M. K. M., Dey, A., Brodwin, M., et al. 2012a, *ApJ*, 752, 86
 Prescott, M. K. M., Dey, A., & Jannuzi, B. T. 2009, *ApJ*, 702, 554
 Prescott, M. K. M., Dey, A., & Jannuzi, B. T. 2012b, *ApJ*, 748, 125
 Prescott, M. K. M., Dey, A., & Jannuzi, B. T. 2013, *ApJ*, 762, 38
 Prescott, M. K. M., Kashikawa, N., Dey, A., & Matsuda, Y. 2008, *ApJ*, 678, L77
 Reuland, M., van Breugel, W., Rütgering, H., et al. 2003, *ApJ*, 592, 755
 Saito, T., Shimasaku, K., Okamura, S., et al. 2006, *ApJ*, 648, 54
 Sanders, D. B., & Mirabel, I. F. 1996, *ARA&A*, 34, 749
 Smail, I., Ivison, R. J., & Blain, A. W. 1997, *ApJ*, 490, L5
 Smith, D. J. B., & Jarvis, M. J. 2007, *MNRAS*, 378, L49
 Smith, D. J. B., Jarvis, M. J., Lacy, M., & Martínez-Sansigre, A. 2008, *MNRAS*, 389, 799
 Smith, D. J. B., Jarvis, M. J., Simpson, C., & Martínez-Sansigre, A. 2009, *MNRAS*, 393, 309
 Steidel, C. C., Adelberger, K. L., Shapley, A. E., et al. 2000, *ApJ*, 532, 170
 Steidel, C. C., Bogosavljević, M., Shapley, A. E., et al. 2011, *ApJ*, 736, 160
 Webb, T. M. A., Yamada, T., Huang, J.-S., et al. 2009, *ApJ*, 692, 1561
 Wright, E. L., Eisenhardt, P. R. M., Mainzer, A. K., et al. 2010, *AJ*, 140, 1868
 Wu, J., Tsai, C.-W., Sayers, J., et al. 2012, *ApJ*, 756, 96
 Yang, Y., Zabludoff, A., Eisenstein, D., & Davé, R. 2010, *ApJ*, 719, 1654
 Yang, Y., Zabludoff, A., Tremonti, C., Eisenstein, D., & Davé, R. 2009, *ApJ*, 693, 1579
 Younger, J. D., Fazio, G. G., Ashby, M. L. N., et al. 2010, *MNRAS*, 407, 1268